



Engineering Optimization

Publication details, including instructions for authors and
subscription information:

<http://www.tandfonline.com/loi/geno20>

Wind farm layout design optimization through multi-scenario decomposition with complementarity constraints

Shen Lu^a & Harrison M. Kim^b

^a Bloomberg LP, 731 Lexington Avenue, New York, NY 10022, USA

^b Industrial and Enterprise Systems Engineering, University of
Illinois at Urbana-Champaign, 104 S. Mathews Avenue, Urbana, IL
61801, USA

Published online: 03 Jan 2014.

To cite this article: Shen Lu & Harrison M. Kim (2014): Wind farm layout design optimization
through multi-scenario decomposition with complementarity constraints, Engineering Optimization,
DOI: [10.1080/0305215X.2013.861457](https://doi.org/10.1080/0305215X.2013.861457)

To link to this article: <http://dx.doi.org/10.1080/0305215X.2013.861457>

PLEASE SCROLL DOWN FOR ARTICLE

Taylor & Francis makes every effort to ensure the accuracy of all the information (the
“Content”) contained in the publications on our platform. However, Taylor & Francis,
our agents, and our licensors make no representations or warranties whatsoever as to
the accuracy, completeness, or suitability for any purpose of the Content. Any opinions
and views expressed in this publication are the opinions and views of the authors,
and are not the views of or endorsed by Taylor & Francis. The accuracy of the Content
should not be relied upon and should be independently verified with primary sources
of information. Taylor and Francis shall not be liable for any losses, actions, claims,
proceedings, demands, costs, expenses, damages, and other liabilities whatsoever or
howsoever caused arising directly or indirectly in connection with, in relation to or arising
out of the use of the Content.

This article may be used for research, teaching, and private study purposes. Any
substantial or systematic reproduction, redistribution, reselling, loan, sub-licensing,
systematic supply, or distribution in any form to anyone is expressly forbidden. Terms &
Conditions of access and use can be found at [http://www.tandfonline.com/page/terms-
and-conditions](http://www.tandfonline.com/page/terms-and-conditions)

Wind farm layout design optimization through multi-scenario decomposition with complementarity constraints

Shen Lu^a and Harrison M. Kim^{b*}

^aBloomberg LP, 731 Lexington Avenue, New York, NY 10022, USA; ^bIndustrial and Enterprise Systems Engineering, University of Illinois at Urbana-Champaign, 104 S. Mathews Avenue, Urbana, IL 61801, USA

(Received 14 November 2012; accepted 15 October 2013)

This article presents a multi-scenario decomposition with complementarity constraints approach to wind farm layout design to maximize wind energy production under region boundary and inter-turbine distance constraints. A complementarity formulation technique is introduced such that the wind farm layout design can be described with a continuously differentiable optimization model, and a multi-scenario decomposition approach is proposed to ensure efficient solution with local optimality. To combine global exploration and local optimization, a hybrid solution algorithm is presented, which combines the multi-scenario approach with a bi-objective genetic algorithm that maximizes energy production and minimizes constraint violations simultaneously. A numerical case study demonstrates the effectiveness of the proposed approach.

Keywords: wind farm; layout optimization; multi-scenario decomposition; complementarity constraints

1. Introduction

Wind power is currently among the fastest growing renewable energy sources worldwide. Motivated by a series of economic, social and political concerns, wind power has received tremendous attention over the past decades and is now considered one of the most promising alternatives to increasingly expensive, rapidly depleting and environmentally controversial fossil energies. Statistics show that the total capacity of wind power installed worldwide increased from 24.3 GW in 2001 to 196.6 GW in 2010 (WWEA Staff 2010), an average growth rate of 25% annually. Such development far exceeds official expectation made at the turn of the century. For example, the wind power capacity installed in Europe was over 86 GW in 2010, more than double the 40 GW originally planned for the year in the European Union's *White Book on Energy*. Assisted by the various institutional supports such as feed-in tariffs (Couture and Gagnon 2010), Kyoto protocol (United Nations 1998), and the White Book (European Commission 1997), wind energy generation has developed to a point where it is not only competitive for meeting small loads at remote locations but also viable for meeting relatively large load demand connected to the grid.

At present time, the rated capacities of wind turbines are still relatively low compared to conventional power generation units. Therefore, to provide more energy, multiple turbines need to be located at a single site, leading to a wind farm. While the integrated deployment of turbines does bring some economic advantage, it also introduces an additional dimension of complexity

*Corresponding author. Email: hmkim@illinois.edu

An earlier version of this article was presented at the 2012 AIAA MAO Conference, Indianapolis, IN, USA.

due to the wake effect: when turbines are placed too close to one another along the prevailing wind direction, the power production of the turbines downstream will be reduced due to the existence of upstream turbines. As a consequence, the layout (*i.e.* the position of the individual turbines) decision of a wind farm has a significant impact on its performance.

The global expansion of wind power generation has been accompanied by rapid development of wind farm layout design methodologies. [Mosetti, Poloni, and Diviacco \(1994\)](#) proposed one of the first optimization approaches for wind turbine placement in a farm setting using a genetic algorithm (GA). A decade later, [Grady, Hussaini, and Abdullah \(2005\)](#) replicated the experiments of [Mosetti, Poloni, and Diviacco \(1994\)](#) by modifying the settings of the GA. Since then, a great number of optimization methods have been presented for wind farm layout design: [Huang \(2007, 2009\)](#) presented improved results on the same case study using a distributed GA that features migration of the fittest individuals among subpopulations; [Wan *et al.* \(2009\)](#) proposed a real-coded GA that allows turbine positions to be adjusted within a computational grid. In addition to GA, [Marmidis, Lazarou, and Pyrgioti \(2008\)](#) introduced a Monte Carlo simulation approach for maximum energy production and minimum installation cost; [Rivas \(2008\)](#) presented a simulated annealing algorithm that involves three turbine placement operations—add, remove and move; [Wan *et al.* \(2010\)](#) proposed a particle swarm algorithm for wind farm layout design optimization with spacing constraints.

In addition to algorithmic developments, a substantial contribution has been made to the wind farm layout design literature from the modelling perspective. In general, the majority of model extensions in wind farm layout design focus on the following aspects: (1) the economic performance of the wind farm; (2) the incorporation of turbine design/selection; (3) the representation of turbine wake; (4) the characterization of wind resource uncertainty; and (5) the consideration of special constraints. For example, [González *et al.* \(2010\)](#) proposed an optimization approach that maximizes the net present value of a wind farm project; [Larsen *et al.* \(2011\)](#) presented a generic economic framework to consider design trade-off in wind farm layout; [Mustakerov and Borissova \(2010\)](#) presented a mixed-integer nonlinear optimization model for wind turbine type and number choice and placement; [Chowdhury *et al.* \(2012b\)](#) considered simultaneous turbine selection and placement using a particle swarm optimization approach; [Lackner and Elkinton \(2007\)](#) developed an analytical framework that integrates wake loss and Weibull wind speed distribution along each direction sector; [Chen and MacDonald \(2011\)](#) proposed a wind farm layout optimization method with consideration of land availability due to the landowner's decision on whether or not to participate in the project; [Cassola *et al.* \(2008\)](#) presented a procedure to calculate the optimal allocation of wind power plants over an extended territory to address the trade-off between wind energy input into the power system and its temporal variability.

This article addresses wind farm layout design optimization with a relatively tight layout and under a limited region size. Limited literature has reported the analysis of the effect of land area (or land use following [Denholm *et al.* 2009](#)). [Christie and Bradley \(2012\)](#) examined the optimal scale of wind turbine arrays that maximizes the power output per unit of land occupied and found that a wind farm designed with this objective could be very different from one designed to maximize economic gain. [Chowdhury *et al.* \(2012a\)](#) presented a response surface model that describes a wind farm's energy production as a function of the land area per megawatt installed (LAMI) and the nameplate capacity of the farm, by sampling the optimal energy production over the LAMI–capacity space. [Denholm *et al.* \(2009\)](#) investigated the land use of 172 US wind farm projects constructed or proposed in the 2000s; their analysis indicates an average land use of 34.5 ± 22.4 hectare/MW from a sample range of 9 to 100 hectare/MW. In this article, a target land-use level that lies at the lower end of this range, *e.g.* around 5 hectare/MW, is considered. For turbine placement in such a setting, inter-turbine spacing is generally more difficult to satisfy. Thus, the computational grid configuration ([Mosetti, Poloni, and Diviacco 1994](#); [Grady, Hussaini, and Abdullah 2005](#); [Marmidis, Lazarou, and Pyrgioti 2008](#); [Huang 2009](#)) commonly employed in

wind farm layout design optimization literature may not be used to ensure inter-turbine spacing. Several grid-free wind farm layout design optimization approaches have been proposed. For example: Kusiak and Zheng (2010) presented a real-coded evolutionary strategy for maximum energy production and minimum constraint violation; Chowdhury *et al.* (2012b) proposed an approach for simultaneous turbine selection and placement, where the latter is handled by a particle swarm algorithm using continuous turbine positions; Kwong *et al.* (2012) introduced a continuous-location model for layout optimization that considers noise propagation as an objective function in addition to energy generation; Du Pont and Cagan (2012) presented an extended pattern search approach which operates with a continuous solution space and employs a random turbine selection mechanism to avoid convergence to local optima.

As of today, almost all the existing approaches for wind farm layout design optimization are based on metaheuristic algorithms. This is partly due to the complexity of the problem: it exhibits a considerable amount of non-smoothness and discreteness, which cannot be easily captured by traditional optimization models based on nonlinear programs. In general, metaheuristic approaches are robust in that they have little requirement on the optimization model's continuous differentiability. In addition, most of them are inherently stochastic and are thus known to possess the capability of global exploration, which may lead to layout designs with better overall performance. However, most of such approaches are also known to lack a guarantee of optimality (Haupt and Haupt 2004), *i.e.* being able to find the exact optimal solution, locally or globally. In addition, some of the metaheuristic approaches may require problem-specific constraint handling strategies to ensure effectiveness of constraint satisfaction (Coello Coello 2002).

This article pursues a different track to address wind farm layout design optimization with the aid of complementarity constraints (CCs). Complementarity is a relationship between functions (variables) where either one (or both) must be at its boundary. An example of a CC is given as follows:

$$\mathbf{0} \leq \mathbf{H}(\mathbf{x}) \perp \mathbf{G}(\mathbf{x}) \geq \mathbf{0}, \quad (1)$$

where \mathbf{x} represents the variables and \mathbf{H} and \mathbf{G} are multifunctions in \mathcal{R}^p . In particular, the symbol \perp indicates that \mathbf{H} and \mathbf{G} are non-negative and that either $[\mathbf{H}]_j$ or $[\mathbf{G}]_j$ or both are zero for $j = 1, \dots, p$. The CC in Equation (1) can be equivalently converted into the following set of inequality constraints:

$$\mathbf{F} \geq \mathbf{0}, \quad \mathbf{G} \geq \mathbf{0}, \quad \mathbf{G}(\mathbf{x}) \circ \mathbf{F}(\mathbf{x}) \leq \mathbf{0}, \quad (2)$$

where the symbol \circ represents the Hadamard product, *i.e.* the term-by-term product operation between two vectors: $\mathbf{a} \circ \mathbf{b} = [a_1, \dots, a_n]^T \circ [b_1, \dots, b_n]^T = [a_1 b_1, \dots, a_n b_n]^T$.

CCs are particularly useful in wind farm layout design optimization since they can be used to capture certain non-smooth wake effect analysis so that the problem is described as a continuously differentiable model. As a result, region boundary and inter-turbine distance constraints can be explicitly handled in the optimization model; and the wind farm layout design optimization problem can be solved through adapting standard gradient-based nonlinear program (NLP) solvers. Importantly, a certain level of local optimality can be ensured from this approach, supported by established theories in mathematical programs with complementarity constraints (MPCCs) (Luo, Pang, and Ralph 1996).

As wind farm layout design optimization usually requires consideration of the farm's performance over a portfolio of wind scenarios (*i.e.* direction and speed) which increases the complexity of the problem, this article also presents a multi-scenario decomposition-based approach to reduce the associated computation. Although most existing approaches in the research area of decomposition-based design optimization are presented for NLP models, the area has recently been linked to MPCCs under the notion of multidisciplinary design optimization with CCs (MDO-CCs) (Lu, Shanbhag, and Kim 2008; Lu and Kim 2010; Lu *et al.* 2010). The presented

decomposition-based approach falls into the context of MDO-CC, and thus can be shown to generate solutions that satisfy certain stationarity conditions.

The complementary properties of the metaheuristic approach and the decomposition-based MDO-CC approach suggest that the two can be combined to achieve better performance. This article proposes to solve the wind farm layout design optimization problem with an approach that hybridizes a GA and a local refinement algorithm based on the presented MDO-CC formulation. The proposed approach combines the global exploration capability of the GA with the local optimization capacity of the MDO-CC approach; it also enables explicit consideration of inter-turbine spacing and regional constraints, as well as the associated sensitivity analysis. The effectiveness of the presented algorithm is demonstrated with a numerical case study.

The article is organized as follows: Section 2 describes a wind farm analysis model, with the calculation of the wake effect and energy production explained. Section 3 presents an optimization model for wind farm layout design, followed by a complementarity reformulation as well as its multi-scenario decomposition formulation. The presented hybrid GA-MDO-CC approach is described in Section 4 and demonstrated with numerical results in Section 5. Conclusions are drawn in Section 6.

2. Performance analysis for wind farm layout design

In this section, the performance analysis of a wind farm is elaborated. Specifically, a wind (direction and speed) distribution model is introduced, followed by the wake effect of wind turbines; after that, the wind distribution and the wake effect are combined to develop a performance assessment model for the wind farm.

2.1. Wind distribution model

The quantity of kinetic energy that a turbine can capture from the wind depends mainly on the wind speed distribution at the turbine site and the power versus wind speed characteristic (also known as the power curve) of the turbine. In this article, it is assumed that the wind speed v at a turbine location is a random variable following a continuous distribution with a probability density function $f_v(v)$ that can be estimated from meteorological data with a distribution identification analysis tool. Many probabilistic models have been proposed to describe wind speed, such as the two-parameter Weibull distribution (Takel and Brown 1978; Skidmore and Tatarko 1990), the two-parameter gamma distribution (Nicks and Lane 1989), and the two-parameter lognormal distribution (Burlaga 2000). Among these models, the two-parameter Weibull distribution is most widely used in wind energy engineering, because it conforms well to the observed long-term distribution of mean wind speeds for a range of sites. On some occasions, the one-parameter Rayleigh distribution, a special case of the Weibull distribution with its shape parameter equal to two, is used to model the wind speed (Corotis, Sigl, and Klein 1978). In this article, it is assumed that the wind speed at a given location follows a two-parameter Weibull distribution, with a scale parameter c and a shape parameter k :

$$f_v(v) = \frac{k}{c} \left(\frac{v}{c}\right)^{k-1} e^{-(v/c)^k}. \quad (3)$$

Moreover, it is assumed that all locations within the terrain under consideration share the same wind direction θ , and that, under each θ , the free-stream wind speed at these locations follows the same Weibull distribution with parameters $c(\theta)$ and $k(\theta)$, where $c(\theta)$ and $k(\theta)$ are functions of θ . This assumption is generally reasonable for a wind farm with relatively flat terrain (Kusiak

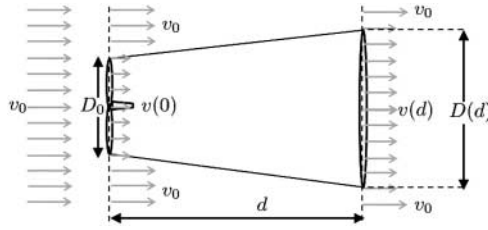


Figure 1. Wake effect of a single turbine.

and Zheng 2010). For regions where this assumption is not satisfied, more complicated wind distribution models need to be applied. For example, Zhang *et al.* (2013) presented a multivariate and multimodal wind distribution that captures the coupled variation of wind speed, wind direction and air density, and showed that such a model provides better estimates than the traditional univariate models such as Weibull, Rayleigh and Gamma distributions. Future work could consider wind farm layout design optimization with more realistic wind distribution models.

2.2. Wake model

As the wind stream flows through the turbine rotor, part of its kinetic energy is captured by the turbine and thus there is a speed loss after the rotor plane. Assuming the flow to be incompressible, the flow stream must be expanded and deflected to keep continuity in the mass flow. This is known as the wake effect of the turbine. As the wind moves downstream, the wake gradually expands and mixes with the surrounding flow, and the wake effect diminishes gradually until the flow speed has fully recovered far downstream (Frandsen *et al.* 2006). The wake effect of a single turbine is illustrated in Figure 1.

Single wake

A wake model is a simplified quantitative means of representing the speed loss and wake expansion. The loss of wind speed due to a turbine wake is usually accounted for by the wind speed deficit, which is defined as the fraction of speed reduction in the wake from the free-stream speed. The speed deficit $dv(d)$ at a distance d downstream from the turbine can be approximated as follows (Lackner and Elkinton 2007):

$$dv(d) = 1 - \frac{v(d)}{v_0} = \begin{cases} \frac{1 - \sqrt{1 - C_T}}{(D_0/D(d))^2} & d > 0 \\ 0 & \text{else.} \end{cases} \quad (4)$$

where v_0 is the free-stream wind speed; $v(d)$ is the wind speed at distance d in the wake; C_T is the thrust coefficient of the turbine; D_0 is the rotor diameter; and $D(d)$ is the wake diameter at distance d downstream. For simplicity of notation, the wind direction θ is dropped from the expressions in the remainder of this subsection unless noted otherwise. Following Katic, Hojstrup, and Jensen (1986), the expansion of the wake can be approximated by a linear model:

$$D(d) = D_0 + 2\kappa d, \quad (5)$$

where κ is the wake decay constant.

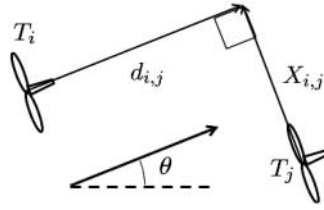


Figure 2. Decomposition of the distance between turbines T_i and T_j .

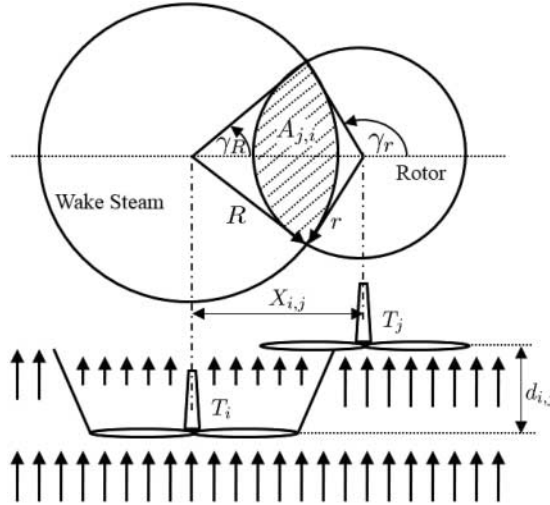


Figure 3. Effect of a partial wake.

Partial wake

The location of a wind turbine T_i is represented by its coordinates (x_i, y_i) in a two-dimensional Cartesian coordinates system. Following this representation, for a given wind direction θ , the distance between the respective rotor planes of two turbines T_i and T_j along θ can be calculated as

$$d_{i,j} = (x_j - x_i) \cos \theta + (y_j - y_i) \sin \theta \quad (6)$$

and the distance $X_{i,j}$ between the two rotor centres along the direction orthogonal to θ can be calculated as

$$X_{i,j} = -(x_j - x_i) \sin \theta + (y_j - y_i) \cos \theta. \quad (7)$$

The two distances are illustrated in Figure 2.

Assuming no other turbines are present, when T_j is fully immersed in the wake of the upstream T_i , the wind speed that reaches T_j 's rotor, v_{j0} , equals the wind speed at $d_{i,j}$ in T_i 's wake, $v_i(d_{i,j})$, which is implied from Equation (4). For the scenarios where T_j is partially immersed in the wake of T_i (as shown in Figure 3), an equivalent wind speed v_{j0} at the rotor plane downstream can be calculated following [González et al. \(2010\)](#):

$$(v_0 - v_{j0})^2 = \frac{A_{j,i}}{A_0} (v_0 - v_i(d_{i,j}))^2, \quad (8)$$

where $A_0 = \pi D_0^2/4$ is the area of T_j 's rotor, and A_{ij} is the overlapping area between T_i 's wake (at distance $d_{i,j}$) and T_j 's rotor:

$$A_{j,i}(R, |X_{i,j}|, r) = \begin{cases} \pi r^2 & |X_{i,j}| \leq R - r, \\ R^2 \left(\gamma_R - \frac{\sin(2\gamma_R)}{2} \right) + r^2 \left(\gamma_r - \frac{\sin(2\gamma_r)}{2} \right) & |X_{i,j}| \in [R - r, R + r], \\ 0 & |X_{i,j}| \geq R + r, \end{cases} \quad (9)$$

where R is the radius of the bigger circumference (usually the wake) and r is the radius of the smaller circumference (usually the rotor); γ_R and γ_r are the central angle corresponding to the overlap at the bigger and smaller circumferences, respectively:

$$\gamma_R = \cos^{-1} \left(\frac{R^2 + X_{i,j}^2 - r^2}{2|X_{i,j}|R} \right) \quad |X_{i,j}| \in [R - r, R + r], \quad (10)$$

$$\gamma_r = \cos^{-1} \left(\frac{R^2 - X_{i,j}^2 - r^2}{2|X_{i,j}|r} \right) \quad |X_{i,j}| \in [R - r, R + r]. \quad (11)$$

Note that Equation (8) can be reformulated as

$$dv_{ji}^2 = \frac{A_{j,i}}{A_0} dv_i^2(d_{i,j}), \quad (12)$$

where dv_{ji}^2 denotes the equivalent wind speed deficit at turbine T_j due to turbine T_i , and $dv_i(d_{i,j})$ denotes the wind speed deficit in the wake of T_i at location $d_{i,j}$.

Multiple wakes

In the wind farm setting, a turbine downstream could be affected by the wakes of multiple turbines upstream. Therefore, the total effect of the wakes needs to be calculated. The reader is referred to [Crespo, Hernandez, and Frandsen \(1999\)](#) for a review of methods that estimate the composite wake effect. In this article, the method by [Katic, Hojstrup, and Jensen \(1986\)](#) is employed. This model indicates that the square of the equivalent wind velocity deficit at a given location can be calculated by superposing the square of the wind velocity deficits induced by all the upstream turbines at this location. Following the model, the expression for the composite wake effect based on the partial wake model in Equation (12) is given by

$$dv_j^2 = \sum_i^N \frac{A_{j,i}}{A_0} dv_i^2(d_{i,j}), \quad (13)$$

where dv_j represents the composite wind speed deficit at turbine T_j 's rotor plane, and N is the total number of turbines.

Once the composite wind speed deficit for a given turbine layout is calculated for a wind direction θ , it can be used to estimate the farm's energy production along θ . This is discussed in Section 2.3.

2.3. Energy production

The power output of a wind turbine can be determined through its power curve $p_w(v)$ and the (equivalent) wind speed that reaches its rotor. As different wind generators have different power

curves, the model used to describe them is also different. Generally speaking, the power output characteristic of a typical wind turbine can be assumed to be such that it starts generating at the cut-in wind speed V_i ; the power output increases as the wind speed increases from V_i to the rated wind speed V_r ; and the rated power p_{wn} is produced when the wind speed varies from V_r to the cut-out wind speed V_o , at which the turbine will be shut down for safety.

This article considers an approximated power curve that describe the turbine's power output in a piecewise linear manner:

$$p_w = \begin{cases} \frac{v - V_i}{V_r - V_i} p_{wn}, & V_i \leq v < V_r \\ p_{wn}, & V_r \leq v \leq V_o \\ 0, & \text{else,} \end{cases} \quad (14)$$

where V_i , V_o and V_r represent the cut-in, the cut-out, and the rated wind speed of the turbine, respectively. Additionally, p_{wn} denotes the rated power of the turbine. Note that although the linear power curve in Equation (14) is just a simplification, the presented approach would also work with any polynomial power curve model.

Following the power curve, the expected total power generated by the wind turbine under a given wind direction can be calculated as

$$\int_{V_i}^{V_o} p_w(v) \frac{k(\theta)}{c(\theta)} \left(\frac{v}{c(\theta)} \right)^{k(\theta)-1} e^{-(v/c(\theta))^{k(\theta)}} dv. \quad (15)$$

The wake effect affects the energy production of a wind turbine through the reduced wind speed at its rotor plane. [Lackner and Elkinton \(2007\)](#) showed that this effect can be accounted for through an equivalent Weibull distribution at the turbine's location. It is also shown that the composite wind speed deficit dv_i at a given turbine T_i only affects the scaling parameter c of the Weibull distribution:

$$c_j(\theta) = (1 - dv_j)c(\theta). \quad (16)$$

Following Equations (15) and (16), the expected total power generated by a wind farm consisting of N identical turbines under wind direction θ can be calculated as

$$E(P(\theta)) = \sum_{j=1}^N \int_{V_{i,j}}^{V_{o,j}} p_{w,j}(v) \frac{k(\theta)}{c_j(\theta)} \left(\frac{v}{c_j(\theta)} \right)^{k(\theta)-1} e^{-(v/c_j(\theta))^{k(\theta)}} dv, \quad (17)$$

where $V_{i,j}$ and $V_{o,j}$ represent the respective cut-in and cut-out wind speeds of turbine T_j , and $p_{w,j}(v)$ is the power curve of T_j .

3. MDO-CC approach for wind farm layout design

In this section, an optimization model for wind farm layout design is presented based on the analysis model summarized in Section 2. To solve the optimization problem, the section first introduces a complementarity reformulation technique which converts the non-smooth wake effect analysis into a set of CCs with continuously differentiable component functions, then presents a multi-scenario decomposition approach that solves the derived optimization model with CCs in a decomposed manner.

3.1. System optimization model

This subsection presents a wind farm layout design optimization model that determines the location of the farm's turbines. Specifically, a wind resource distribution characterized by n scenarios, $\omega^{(1)}, \dots, \omega^{(n)}$, is considered, with each scenario $\omega^{(m)}$ defined a

$$\{\omega^{(m)} | \theta^{(m)}, \Pr^{(m)}\}, \quad (18)$$

where $\theta^{(m)}$ denotes the wind direction under scenario $\omega^{(m)}$ and $\Pr^{(m)}$ denotes $\omega^{(m)}$'s frequency of appearance. The problem is set up such that it locates N homogenous turbines to maximize the energy production of the farm. The formulation of the wind farm layout design optimization (WFLDO) problem is given as

$$\text{WFLDO : } \max_{x_1, \dots, x_N, y_1, \dots, y_N} \left(\sum_{m=1}^n \Pr^{(m)} \cdot E(P(\theta^{(m)})) \right) \cdot T_Y \quad (19a)$$

$$\text{s.t. } x_i^2 + y_i^2 \leq R_c^2, \quad \forall i = 1, \dots, N, \quad (19b)$$

$$(x_i - x_j)^2 + (y_i - y_j)^2 \geq (\alpha \cdot D_0)^2, \quad \forall i, j = 1, \dots, N, \quad i \neq j, \quad (19c)$$

where x_i and y_i denote the two-dimensional coordinates of turbine T_i , R_c denotes the radius of the terrain in consideration, D_0 is the rotor radius of the turbines, α is a spacing factor that specifies the minimum inter-turbine distance, $E(P(\theta^{(m)}))$ is calculated from Equation (17), based on the wake effect model in Section 2, and $T_Y = 365 \times 24$ represents the number of hours per year. Equation (19b) requires that all the turbines should be placed within the terrain in consideration. While a circular terrain is considered in this chapter, other two-dimensional analytical geometric shapes can be easily considered. In addition, Equation (19c) indicates a minimum technical distance between each pair of turbines in a multiple of the rotor diameter. Ensuring sufficient spacing reduces interactions such as turbulence, thus diminishing hazardous loads on the turbine. It also ensures the quality of the wake model in the previous subsection as accuracy decreases at the near-wake phase. The factor α may be determined based on empirical knowledge as well as the characteristics of the wind distribution, the turbine and the terrain.

The objective of Equation (19) does not explicitly consider the cost of energy production. Here, the assumption is that the cost of energy (COE) is affected by the energy production following Walford (2006):

$$\text{COE} = \frac{C_I \cdot \text{FCR} + C_R}{\text{AEP}} + C_{\text{O\&M}}, \quad (20)$$

where C_I is the initial capital cost, FCR is the annual fixed charge rate, C_R is the levelized replacement cost, $C_{\text{O\&M}}$ is the maintenance and operation cost of energy, and AEP is the expected annual energy production. In other words, given that the other terms are fixed, COE can be reduced by maximizing the expected energy production. Note that Equation (20) is only a simplified relation between COE and energy production. Future research could consider wind farm layout design for COE optimization with a more accurate cost model.

3.2. Complementarity reformulation of the wake effect

Although the wind farm layout design optimization model presented in Equation (19) is straightforward, the calculation of the objective function is based on the wake effect analysis model in Section 2, part of which (e.g. Equations 4 and 9) are non-smooth. Thus, efficient gradient-based NLP algorithms cannot be directly applied to solve the optimization problem in Equation (19). Traditionally, one way of handling such an optimization model is to apply gradient-free heuristic

approaches such as genetic algorithms. While this type of approach is robust in general, it also suffers from the lack of guarantees for optimality.

In this subsection, a different track for handling the discreteness is presented through the aid of CCs: the non-smooth wake effect analysis is reformulated into a set of CCs. With this reformulation, the resulting optimization model is continuously differentiable, and standard NLP solvers can be adapted to solve the problem efficiently with a certain level of local optimality guaranteed by established theories in mathematical programs with complementarity constraints (MPCCs).

3.2.1. Complementarity reformulation of non-smooth functions

Consider a continuous piecewise smooth function $F(\mathbf{x})$ that is a generalization of the non-smooth functions in Equations (4) and (9):

$$F(\mathbf{x}) = F_i(\mathbf{x}), \quad \text{if } \tau_{i-1} \leq \varphi(\mathbf{x}) \leq \tau_i, \quad \forall i = 1, \dots, m, \quad (21)$$

where $\varphi(\mathbf{x})$ is a switching function; $F_i(\mathbf{x})$ is a smooth function over $\varphi(\mathbf{x})$'s range; and $\tau_0 \leq \tau_1 \leq \dots \leq \tau_m$ are the switching thresholds. The function has an implicit aspect of discrete selection as it switches between adjacent intervals. In order to facilitate formulation, this article represents the piecewise function as a smooth optimization problem below. Note that the 'if' statement in Equation (21) is converted to a smooth minimization problem; and F obtained through Equation (22) has the same value as that obtained by (21) for any \mathbf{x} .

$$\begin{aligned} F(\mathbf{x}) &= \sum_{i=1}^m F_i(\mathbf{x})z_i, \\ \min_{z_i} \quad &\sum_{i=1}^m (\varphi(\mathbf{x}) - \tau_{i-1})(\varphi(\mathbf{x}) - \tau_i)z_i, \\ \text{s.t.} \quad &\sum_{i=1}^m z_i = 1, \\ &z_i \geq 0. \end{aligned} \quad (22)$$

Note that there is no integer requirement on the z_i 's, while they take only discrete values in the optimal solution of (22). The discrete selection is implicitly taken care of by the optimization problem. Replacing the optimization problem (22) with its optimality conditions, which are in the format of CCs, the piecewise smooth function is converted into its complementarity reformulation:

$$\begin{aligned} F(\mathbf{x}) &= \sum_{i=1}^m F_i(\mathbf{x})z_i, \\ (\varphi(\mathbf{x}) - \tau_{i-1})(\varphi(\mathbf{x}) - \tau_i) - \gamma - s_i &= 0, \\ 0 \leq z_i \perp s_i &\geq 0, \\ \sum_{i=1}^m z_i &= 1, \end{aligned} \quad (23)$$

where γ and s_i represent the Lagrange multipliers corresponding to the summation and non-negativity constraints, respectively. Note that the z_i 's may take fractional values when φ is equal to one of the thresholds. This problem is trivial when the piecewise function is continuous at the switching points.

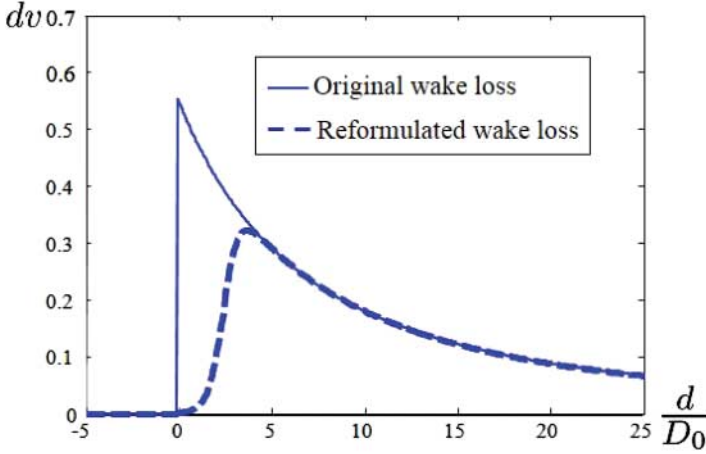


Figure 4. Reformulation of single wake speed loss: $C_T = 0.8$, $\kappa = 0.075$, $a = 2.5$, $b = 2.5$.

3.2.2. Reformulation of single wake speed loss

It can be noted that the mathematical expression for single wake speed loss $dv(d)$ in Equation (4) is not a continuous function at $d = 0$. This is intuitive in a physical sense in that the speed deficit is zero for any point in front of the rotor, while it becomes most prominent immediately after the rotor (as illustrated by the solid curve in Figure 4). Although such discontinuities are usually difficult to approximate with smooth functions, the existence of the inter-turbine distance constraints (Equation 19c) in practice makes the near-rotor wake effect irrelevant to wind farm layout design optimization. As a result, a smooth function can be employed to approximate the discontinuous single wake speed loss. In general, this approximation is not likely to affect the quality of wake loss analysis as long as it provides enough accuracy in feasible regions of the inter-turbine distance constraints.

As a first step in reformulating Equation (4), a pair of complementary surplus and slack variables, s_1 and s_2 , are introduced such that they satisfy the following:

$$\begin{aligned} d - s_1 + s_2 &= 0, \\ 0 &\leq s_1 \perp s_2 \geq 0. \end{aligned} \quad (24)$$

Since s_1 equals the maximum of d and zero, Equation (4) can be simplified by replacing d with s_1 . The resulting expression is shown as follows:

$$dv(d) = \frac{1 - \sqrt{1 - C_T}}{(D_0/D(s_1))^2}. \quad (25)$$

Note that the negative case of Equation (4) is implicitly captured by the complementarity constraint, therefore it is no longer needed.

Finally, the approximation of the discontinuous single wake speed loss is fulfilled through introducing a logistic function:

$$l(s_1) = \frac{1}{1 + e^{-a(s_1 - b)}}. \quad (26)$$

This function features a smooth transition from zero to one, the ‘slope’ and position of which are controlled by parameters a and b , respectively. The values of the two parameters are chosen based on the multiplier α in the inter-turbine spacing constraint. The reformulated speed loss in

Equation (25) is multiplied by the logistic function to create the approximation. As a result, the product of the multiplication would be a close approximation to the original speed loss function for sufficiently large s_1 . The complete reformulation of Equation (4) (as illustrated by the dashed curve in Figure 4) is given as

$$\begin{aligned}\tilde{d}v(s_1) &= \frac{1 - \sqrt{1 - C_T}}{(D_0/D(s_1))^2} l(s_1), \\ d - s_1 + s_2 &= 0, \\ 0 \leq s_1 \perp s_2 &\geq 0.\end{aligned}\tag{27}$$

3.2.3. Reformulation of the partial wake overlap

In order to reformulate the expression for the overlapping area $A_{j,i}$ (Equation 9) in the partial wake analysis model, it is first noted that $A_{j,i}$ is a twice-continuously differentiable function of R , r and $|X_{i,j}|$. This can be easily seen through calculating the limits of the $A_{j,i}$'s first and second derivatives at $|X_{i,j}| = R - r$ and $|X_{i,j}| = R + r$, respectively. Thus its proof will be omitted. To capture the non-smooth absolute value, a pair of complementary surplus and slack variables, s_3 and s_4 , are introduced, such that they satisfy the following:

$$\begin{aligned}X_{i,j} - s_3 + s_4 &= 0, \\ 0 \leq s_3 \perp s_4 &\geq 0.\end{aligned}\tag{28}$$

As a result, $s_3 + s_4$ can be used to replace $|X_{i,j}|$ in Equation (9):

$$A_{j,i}(R, |X_{i,j}|, r) = A_{j,i}\left(\frac{D(d_{i,j})}{2}, s_3 + s_4, \frac{D_0}{2}\right).\tag{29}$$

Note that R and r are also replaced by $D(d_{i,j})/2$ and $D_0/2$, respectively, since the wake is always the larger circumference in Figure 3 for the homogenous turbine case. Equations (28) and (29) provide the complete reformulation of the overlapping area $A_{j,i}$ in the partial wake analysis model.

3.2.4. Complementarity reformulation of the wind farm layout design optimization

As a summary of this subsection, the complementarity reformulation of the wind farm layout design optimization problem is presented, which is derived by applying the presented reformulation technique to the interaction of each pair of turbines. The formulation is given as follows:

$$\begin{aligned}\text{WFLDO}_{\text{AIO}} : & \max \left(\sum_{m=1}^n \text{Pr}^{(m)} \cdot E(P(\theta^{(m)})) \right) \cdot T_Y \\ \text{w.r.t. } & x_i, y_i, \forall i = 1, \dots, N, s_{j,i,1}^{(m)}, s_{j,i,2}^{(m)}, s_{j,i,3}^{(m)}, s_{j,i,4}^{(m)}, \forall m = 1, \dots, n, \forall i, j = 1, \dots, N, i \neq j \\ & \text{s.t. } x_i^2 + y_i^2 \leq R_c^2, \forall i, \\ & (x_i - x_j)^2 + (y_i - y_j)^2 \geq (\alpha \cdot D_0)^2, \forall i, j, i \neq j, \\ & (x_j - x_i) \cos \theta^{(m)} + (y_j - y_i) \sin \theta^{(m)} - s_{j,i,1}^{(m)} + s_{j,i,2}^{(m)} = 0, \forall m, \forall i, j, i \neq j,\end{aligned}\tag{30}$$

$$\begin{aligned}
& -(x_j - x_i) \sin \theta^{(m)} + (y_j - y_i) \cos \theta^{(m)} - s_{j,i,3}^{(m)} + s_{j,i,4}^{(m)} = 0, \quad \forall m, \forall i, j, i \neq j, \\
c_j(\theta^{(m)}) = c(\theta^{(m)}) & \left(1 - \sqrt{\sum_{i=1, i \neq j}^N \frac{A_{j,i} \left(\frac{D(s_{j,i,1}^{(m)})}{2}, s_{j,i,3}^{(m)} + s_{j,i,4}^{(m)}, \frac{D_0}{2} \right)}{D_0^2/2}} \tilde{d}v^2(s_{i,j,1}^{(m)})} \right) \forall m, \forall i, j, i \neq j,
\end{aligned}$$

where the relation between $c_j(\theta^{(m)})$ and the objective is dictated by Equation (17). Since $c_j(\theta^{(m)})$ is an intermediate result rather than a constraint, the corresponding equality will be dropped from any subsequent optimization formulations. The above formulation is referred to as the all-in-one (AIO) complementarity formulation, as all the design variables are handled in a single optimization problem.

3.3. Decomposed formulation

It is noted that the formulation in Equation (30) is twice-continuously differentiable. Therefore it can be directly solved with various continuous MPCC solvers in an AIO manner. The idea behind AIO approaches is straightforward; however, the scenario-specific interaction variables increase the size of the problem, and generally make the direct solution of the AIO problem inefficient. An alternative to the AIO approach is a decomposition-based approach [Balling and Sobieszcanski-Sobieski \(1996\)](#), where the original AIO problem is decomposed into a set of interrelated subproblems, and solved through an iterative process of subproblem optimization and coordination among them. Using the decomposition-based approach can be advantageous, as it decomposes the AIO problem into smaller subproblems that are usually easier to solve while limiting the communication among subproblems only to where necessary via linking variables.

Although most existing approaches in the research area of decomposition-based design optimization are presented for NLP models, the research area has recently connected to MPCCs under the notion of MDO-CC. [Lu, Shanbhag, and Kim \(2008\)](#) formally stated the research problem of MDO-CC and presented an augmented Lagrangian decomposition (ALD) approach, with the connection between the stationarity conditions of the decomposed formulation and those of the AIO formulation established; [Lu and Kim \(2010\)](#) proposed a regularized inexact penalty decomposition approach for MDO-CC and showed that existing theories can be adapted to show convergence of the presented algorithm.

In derivation of a decomposed formulation, the augmented Lagrangian decomposition (ALD) approach [Lu, Shanbhag, and Kim \(2008\)](#) is followed: the two-dimensional coordinates of each turbine x_i and y_i are taken as linking variables; a local copy of the linking variables, $x_i^{(m)}$ and $y_i^{(m)}$, is first introduced to each relevant scenario k , together with a set of consistency constraints; then the consistency constraints are relaxed, and the corresponding violation is penalized in the objective function through inconsistency variables; after that, the problem is decomposed into a bi-level formulation composed of a system level coordination problem and a subsystem level coordination problem including n separated individual scenario subproblems. The m th scenario of the multi-scenario decomposed formulation is given as

$$\begin{aligned}
& \text{WFLDO}_{\text{sub},m} : \max (\text{Pr}^{(m)} \cdot E(P(\theta^{(m)}))) \cdot T_Y + \varepsilon^{(m)} \\
& \text{w.r.t. } \varepsilon^{(m)}, \quad x_i^{(m)}, y_i^{(m)}, \quad \forall i = 1, \dots, N, \quad s_{j,i,1}^{(m)}, s_{j,i,2}^{(m)}, s_{j,i,3}^{(m)}, s_{j,i,4}^{(m)}, \quad \forall i, j = 1, \dots, N, i \neq j \\
& \text{s.t. } \quad (x_i^{(m)})^2 + (y_i^{(m)})^2 \leq R_c^2, \quad \forall i,
\end{aligned} \tag{31}$$

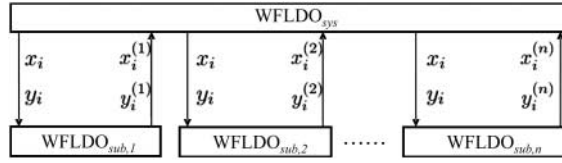


Figure 5. Decomposed problem structure of wind farm layout design optimization.

$$\begin{aligned}
 & \left(x_i^{(m)} - x_j^{(m)}\right)^2 + \left(y_i^{(m)} - y_j^{(m)}\right)^2 \geq (\alpha \cdot D_0)^2, \quad \forall i, j, i \neq j, \\
 & \left(x_j^{(m)} - x_i^{(m)}\right) \cos \theta^{(m)} + \left(y_j^{(m)} - y_i^{(m)}\right) \sin \theta^{(m)} - s_{j,i,1}^{(m)} + s_{j,i,2}^{(m)} = 0, \quad \forall i, j, i \neq j, \\
 & -\left(x_j^{(m)} - x_i^{(m)}\right) \sin \theta^{(m)} + \left(y_j^{(m)} - y_i^{(m)}\right) \cos \theta^{(m)} - s_{j,i,3}^{(m)} + s_{j,i,4}^{(m)} = 0, \quad \forall i, j, i \neq j, \\
 & \varepsilon^{(m)} \geq \sum_{i=1}^N \left[v_{i,x}^{(m)} \left(x_i - x_i^{(m)}\right) + w_{i,x}^{(m)} \left(x_i - x_i^{(m)}\right)^2 + v_{i,y}^{(m)} \left(y_i - y_i^{(m)}\right) + w_{i,y}^{(m)} \left(y_i - y_i^{(m)}\right)^2 \right],
 \end{aligned}$$

where $\varepsilon^{(m)}$ is an inconsistency variable to maintain the regularity condition of the deviation constraints [Sobieszcanski-Sobieski \(1995\)](#). The inconsistency between linking variables is penalized by the augmented Lagrangian penalty function: $w_{i,x}$ and $w_{i,y}$ are the respective weight factors assigned to consistency constraints $x_i - x_i^{(m)} = 0$ and $y_i - y_i^{(m)} = 0$; $v_{i,x}$ and $v_{i,y}$ are estimations of the respective Lagrange multipliers corresponding to the two consistency constraints.

The formulation of the upper level coordination problem is given as

$$\begin{aligned}
 & \text{WFLDO}_{\text{sys}} : \min \quad \varepsilon \\
 & \text{w.r.t. } x_i, y_i, \varepsilon \\
 & \text{s.t. } \varepsilon \geq \sum_{m=1}^n \left\{ \sum_{i=1}^N \left[v_{i,x}^{(m)} \left(x_i - x_i^{(m)}\right) + w_{i,x}^{(m)} \left(x_i - x_i^{(m)}\right)^2 + v_{i,y}^{(m)} \left(y_i - y_i^{(m)}\right) + w_{i,y}^{(m)} \left(y_i - y_i^{(m)}\right)^2 \right] \right\}.
 \end{aligned} \tag{32}$$

The decomposed problem structure is illustrated in [Figure 5](#). In the next section, a solution algorithm based on the above MDO-CC decomposed formulation will be presented to solve the original wind farm layout design optimization problem.

4. Hybrid solution algorithm

It is noted that the MDO-CC decomposed formulation presented in [Equations \(31\) and \(32\)](#) is twice-continuously differentiable and can thus be solved by decomposition-based MDO-CC approaches [Lu, Shanbhag, and Kim \(2008\)](#), [Lu and Kim \(2010\)](#). Generally, these approaches can generate locally optimal layouts in a continuous setting; they also directly handle constraints such as minimum inter-turbine distance and region boundary for the case where compact layouts are expected. However, these approaches are not developed to obtain global optimal solutions. On the other hand, traditional metaheuristic approaches, as discussed in [Section 1](#), are known for their capacity of global exploration, but also that they suffer from lack of guarantees of optimality as well as inefficient constraint handling. The foregoing discussion highlights the complementary properties of GAs and the MDO-CC approach, and suggests a solution algorithm in the form of a hybridization between the two approaches. In this section, a hybrid solution algorithm that combines a bi-objective GA and a decomposition-based MDO-CC local refinement approach

is presented to solve the wind farm layout design optimization problem. The MDO-CC local refinement approach is described in Section 4.1; the bi-objective GA employed is explained in Section 4.2; and the hybridization scheme is presented in Section 4.3.

4.1. Decomposition-based MDO-CC local refinement approach

As can be noted in Equations (31) and (32), the MDO-CC decomposed formulation of wind farm layout design optimization is parameterized by weighting factors. Solving the decomposed problem under fixed weights does not usually lead to feasible solutions of the original AIO problem. Therefore, a weight updating scheme is necessary so that the successive solutions of the decomposed formulation converge to an optimal solution of the original AIO problem.

The presented decomposition-based MDO-CC local refinement approach follows the alternating direction method of multipliers Bertsekas (2003), Tosserams, Etman, and Rooda (2007): in each iteration, the individual scenario subproblems in Equation (31) are first solved either sequentially or in parallel under fixed penalty parameters; then the system (upper) level coordination problem in Equation (32) is solved under the same penalty parameter settings. After that, the penalty parameters are updated based on the violation of the linking variable consistencies. Under the augmented Lagrangian formulation, the violation of the consistency constraints, $x_i - x_i^{(m)} = 0$ and $y_i - y_i^{(m)} = 0$, can be reduced by taking the corresponding Lagrange multiplier estimates, $v_{i,x}^{(m)}$ and $v_{i,y}^{(m)}$, close to their values associated with the optimal AIO solution. In order to achieve this, a linear updating scheme for selecting $v_{i,x}^{(m)}$ and $v_{i,y}^{(m)}$ is given by

$$\begin{aligned} (v_{i,x}^{(m)})^{(k+1)} &= (v_{i,x}^{(m)})^{(k)} + 2(w_{i,x}^{(m)})^{(k)}(w_{i,x}^{(m)})^{(k)}(x_i - x_i^{(m)})^{(k)}, \quad \forall m, i, \\ (v_{i,y}^{(m)})^{(k+1)} &= (v_{i,y}^{(m)})^{(k)} + 2(w_{i,y}^{(m)})^{(k)}(w_{i,y}^{(m)})^{(k)}(y_i - y_i^{(m)})^{(k)}, \quad \forall m, i, \end{aligned} \quad (33)$$

where the superscript (k) indicates the value of a variable or an expression at the k th iteration. Additionally, the weight factors are updated following a linear growth formula:

$$\begin{aligned} (w_{i,x}^{(m)})^{(k+1)} &= \beta \cdot (w_{i,x}^{(m)})^{(k)}, \quad \forall m, i, \\ (w_{i,y}^{(m)})^{(k+1)} &= \beta \cdot (w_{i,y}^{(m)})^{(k)}, \quad \forall m, i, \end{aligned} \quad (34)$$

where β is a growth factor.

The iteration is terminated when the following condition is satisfied:

$$\frac{\sum_{m=1}^n \|\mathbf{z} - \mathbf{z}^{(m)}\|_2^2}{1 + \|\mathbf{z}\|_2} < \epsilon_{\text{tol}} \quad (35)$$

where $\mathbf{z} = [x_1, \dots, x_N, y_1, \dots, y_N]$ is the system level value of the linking variables, $\mathbf{z}^{(m)} = [x_1^{(m)}, \dots, x_N^{(m)}, y_1^{(m)}, \dots, y_N^{(m)}]$ is the subsystem level value of the linking variables, and ϵ_{tol} is a tolerance parameter. The solution algorithm is illustrated in Figure 6.

4.2. A bi-objective genetic algorithm for wind farm layout design optimization

This subsection describes the GA employed to solve the wind farm layout design optimization problem. The solution representation is first stated, followed by a constraint handling mechanism. Then, the flow of the algorithm is stated, and the genetic operators are addressed.

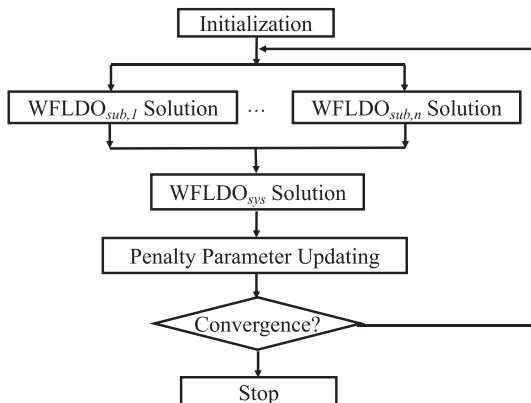


Figure 6. Alternating direction approach for MDO-CC local refinement.

Solution representation

A solution, referred to as an individual, to the original wind farm layout design optimization problem in Equations (19) is represented by a binary string composed of N substrings:

$$\mathbf{bx} = (bx_1, by_1, \dots, bx_N, by_N), \quad (36)$$

where bx_i, by_i are two binary substrings of l_b bits each, representing a fraction number between zero and one, respectively. The two fraction numbers are converted to the coordinates of a turbine, using the upper and lower bounds of the x - and y -coordinates. For example, let ex_i be the fraction represented by bx_i , then x_i is calculated as

$$x_i = x_{\min} + ex_i \cdot (x_{\max} - x_{\min}), \quad (37)$$

where x_{\min} and x_{\max} are the minimum and maximum x -coordinate values of the feasible region. Note that this representation does not assume a grid layout, as do most GAs for wind farm layout design. Therefore the constraints must be handled explicitly to ensure feasibility. The value of l_b may depend on the expected accuracy as well as the compactness of the farm: if a more compact layout is required, higher accuracy might be necessary to facilitate constraint handling.

Constraint handling mechanism

A constraint handling mechanism is introduced in the GA following a typical bi-objective setting. Specifically, the maximization of wind energy production and the minimization of constraint violation are considered as two conflicting objectives. For simplicity of notation, the maximization of wind energy production is converted into the minimization of its negative, so that both objectives are to be minimized. The objectives are stated as follows:

$$\min \{O_1(\mathbf{bx}), O_2(\mathbf{bx})\}, \quad (38)$$

where

$$O_1(\mathbf{bx}) = - \sum_{m=1}^n \Pr^{(m)} \cdot E(P(\theta^{(m)})), \quad (39)$$

$$O_2(\mathbf{bx}) = \sum_{i=1}^N \max\{0, (x_i^2 + y_i^2 - R_c^2)\} + \sum_{i=1}^N \sum_{j=1, j \neq i}^N \max\{0, [(c \cdot D_0)^2 - (x_i - x_j)^2 + (y_i - y_j)^2]\}. \quad (40)$$

In order to handle the constraints, an elite set is introduced to approximate the Pareto frontier that characterizes the trade-off between the two objectives. In the process of optimization, the elite set is updated in each iterate through inserting all the non-dominated individuals from the population into the set and removing all the dominated individuals from the set. Here, an individual \mathbf{bx}_1 dominates another individual \mathbf{bx}_2 , represented as $\mathbf{bx}_1 > \mathbf{bx}_2$, if the following conditions are satisfied:

$$O_1(\mathbf{bx}_1) \leq O_1(\mathbf{bx}_2), \quad O_2(\mathbf{bx}_1) \leq O_2(\mathbf{bx}_2), \quad (41a)$$

$$O_1(\mathbf{bx}_1) < O_1(\mathbf{bx}_2) \quad \text{or} \quad O_2(\mathbf{bx}_1) < O_2(\mathbf{bx}_2). \quad (41b)$$

An individual is called non-dominated if it is not dominated by any of the individuals evaluated so far.

Algorithm description

The GA employed for wind farm layout design optimization is described in Algorithm 1. Here, two terminating criteria are considered: the maximum number of iterations gen_{\max} and the maximum number of iterations without improvement $gen_{nImp, \max}$. The algorithm is terminated when either criterion is satisfied.

BEGIN

Step 0: Initialize empty parent set S_P , population S_0 and elite set S_E ; randomly generate N_0 individuals to fill S_0 ; $gen = 1$; $gen_{nImp} = 0$; $\mathbf{bx}_{\min} = \{\}$

Step 1: **REPEAT**

Step 1.1: Insert all the non-dominated solutions in S_0 into S_E ;
remove dominated solutions from S_E .

Step 1.2: Assign fitness to individuals in S_E and S_0 .

Step 1.3: Select N_P individuals from S_0 and S_E to fill S_P .

Step 1.4: Generate N_0 new individuals to form the new population S_0 ,
each by applying crossover to two individuals randomly selected
from S_P , with probability P_X .

Step 1.5: Mutate each individual in S_0 , with probability P_M .

Step 1.6: Find the individual \mathbf{bx}^* with the minimum O_2 ;

IF $\mathbf{bx}_{\min} = \{\}$ **OR** $O_2(\mathbf{bx}^*) < O_2(\mathbf{bx}_{\min})$,

THEN $\mathbf{bx}_{\min} = \mathbf{bx}^*$; $gen_{nImp} = 0$.

ELSEIF $O_1(\mathbf{bx}^*) < O_1(\mathbf{bx}_{\min})$ **AND** $O_2(\mathbf{bx}^*) < O_2(\mathbf{bx}_{\min}) * (1 + \varepsilon_{tol})$

THEN $\mathbf{bx}_{\min} = \mathbf{bx}^*$; $gen_{nImp} = 0$.

ELSE $gen_{nImp} = gen_{nImp} + 1$.

Step 1.7: $gen = gen + 1$

UNTIL $gen > gen_{\max}$ **OR** $gen_{nImp} = gen_{nImp, \max}$

END

Fitness assignment

The fitness of an individual \mathbf{bx} in the elite set S_E is defined as

$$\text{fitness}(\mathbf{bx}) = \frac{N_I(\mathbf{bx})}{N_O}, \quad (42)$$

where $N_I(\mathbf{bx})$ denotes the number of individuals in the population S_O , which is dominated by \mathbf{bx} . After fitness values have been assigned to all the individuals in the elite set S_E , the fitness of an individual \mathbf{bx}' in the population S_O is then defined as

$$\text{fitness}(\mathbf{bx}') = \sum_{\mathbf{bx} \in S_E, \mathbf{bx} > \mathbf{bx}'} \text{fitness}(\mathbf{bx}) + 1, \quad (43)$$

where the first term on the right-hand side is the sum of the fitness of all the individuals in S_E that dominate \mathbf{bx} . The value one is added to ensure that individuals in the elite set S_E have a better fitness than individuals in the population S_O .

The combination of the constraint handling mechanism and fitness assignment method employed is also known as the strength Pareto approach. The approach has been applied to an evolutionary strategy algorithm by [Zitzler and Thiele \(1999\)](#).

Crossover, mutation and selection

Both the crossover and mutation are performed on a substring basis, *i.e.* they are applied between each corresponding pair of substrings. A standard two-point crossover operator and a bit mutation operator are employed. The two operators are applied with a crossover probability P_X and a mutation probability P_M , respectively.

In addition, a tournament selection with replacement of size N_T is employed to qualify individuals for reproduction: N_T individuals are selected randomly, and the individual with the best fitness value is inserted into S_P .

4.3. Hybridization scheme

The MDO-CC local refinement algorithm is combined with the above described GA in the following manner: when the maximum number of iterations without improvement $gen_{nImp, \max}$ is reached, the local refinement is applied to the N_R most feasible individuals in the elite set S_E . The solution with best objective value from the local refinements is translated into an individual \mathbf{bx}^* which is then compared with the most feasible individual in the elite set \mathbf{bx}_{\min} . If the following criteria are satisfied:

$$O_2(\mathbf{bx}^*) < O_2(\mathbf{bx}_{\min}) \quad \text{or} \quad O_1(\mathbf{bx}^*) < O_1(\mathbf{bx}_{\min}) \cdot (1 + \varepsilon_{\text{tol}}), \quad (44)$$

then \mathbf{bx}^* is inserted into the elite set S_E ; after that, all the dominated individuals in the elite set S_E are removed from the set and the GA continues with a zero gen_{nImp} . Note that a truncation error may occur when a solution is translated to an individual. If Equation (44) fails, then the GA terminates. Figure 7 shows an overall flowchart of the presented solution algorithm, including the GA and the local refinement.

5. Numerical case study

In this section, a numerical study based on an illustrative wind farm is presented to demonstrate the presented decomposition-based MDO-CC approach as well as the hybrid optimization algorithm.

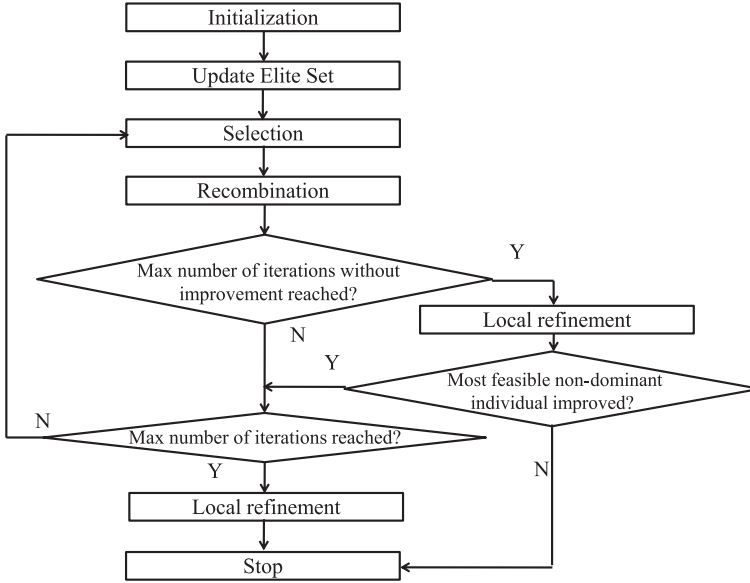


Figure 7. Flowchart of the presented hybrid GA-MDO-CC approach.

Table 1. Distribution of wind direction and speed considered for the illustrative case.

m	$\theta^{(m)}$	$k(\theta^{(m)})$	$c(\theta^{(m)})$	$p^{(m)}$
1	30°	2	7	0.2
2	90°	2	5	0.16
3	150°	2	5	0.16
4	210°	2	5	0.16
5	270°	2	5	0.16
6	330°	2	4	0.16

5.1. Illustrative case

This subsection considers an illustrative case in which 10 identical turbines are to be placed within a circumference of radius $R_c = 500$ m. The diameter of the turbines' rotor plane $D_0 = 77$ m and the spacing factor for minimum inter-turbine spacing is $\alpha = 4$. Apparently, such a parameter setting requires a compact layout of turbines; hence the constraint handling is not a trivial issue. Other parameters of the wind turbine are given as follows: rated capacity $p_{wn} = 1500$ kW; cut-in wind speed $V_i = 3.5$ m/s; rated wind speed $V_r = 14$ m/s; cut-out wind speed $V_o = 23.5$ m/s; hub height $z = 80$ m; trust coefficient $C_T = 0.8$; and decay constant of the wake $\kappa = 0.075$. The wind scenario shown in Table 1 is considered. To facilitate the calculation of wind energy production, a numerical integration is conducted with a speed interval of 0.5 m/s.

5.2. Numerical results

The illustrative case described above is used to test the presented MDO-CC local refinement approach as well as the presented hybrid GA-MDO-CC algorithm. Specifically, the MDO-CC approach is first verified through comparing its results with those of an MPCC solver applied to the AIO complementarity formulation; then the optimization results from the proposed hybrid

GA-MDO-CC algorithm are presented in order to demonstrate its effectiveness; after that, the results of a sensitivity analysis performed on one of the solutions obtained is provided for insight into the layout design problem.

MDO-CC local refinement algorithm

The first numerical study is conducted to show the numerical behaviour of the presented MDO-CC approach. The MDO-CC approach is applied to solve the wind farm layout design optimization problem in the illustrative case study from 10 randomly generated initial points. Numerical results indicate that, for each initial solution tested, the MDO-CC approach converges to a solution identical to a local optimal solution to the AIO complementarity formulation in Equation (30). The local optimality of the solutions obtained is numerically verified by feeding their corresponding AIO solution to an MPCC solver applied to the AIO complementarity formulation. Here both the AIO problem and the subproblems of the MDO-CC approach are solved with the KNITRO[®] 5.0 solver in a MATLAB[®] 7.4 environment. The program runs on an Intel Core 2 Duo CPU 3.16 GHz, 4 GB memory. The MDO-CC approach employs a β -value of 1.1.

In addition, the KNITRO solver is used to solve the AIO formulation from the same set of initial points against which the MDO-CC approach is tested. It can be noted that the AIO approach and the MDO-CC approach may converge to different solutions when applied to the same initial solution; however, both solutions are locally optimal. The average computation times associated with the two algorithm are compared in Table 2. This table indicates that the average computation time taken by the MDO-CC approach is approximately a third of that taken by the AIO MPCC approach; this result is obtained when the number of wind scenarios in the illustrative case is six. Here, the computation time of the MDO-CC approach is measured under serial implementation, *i.e.* the computation time is the summation of all the subsystem computation times. A parallel implementation will generally lead to more computational savings.

Optimization results

A second numerical study is performed to verify the presented hybrid GA-MDO-CC optimization algorithm. The algorithm is applied to the illustrative case study for 10 executions, all of which generated feasible solutions to the case problem. The average performance of the algorithm is presented in Table 3. For verification purposes, the problem is also solved by the GA presented in Section 4.2 without the MDO-CC local refinement. The GA was tested for 20 trials, 9 of which generated feasible solutions. Of the 9 successful executions, the average energy production and

Table 2. Average computation times associated with the MDO-CC approach and the AIO MPCC approach.

Solution algorithm	MDO-CC	AIO MPCC
Average computation time (s)	964.6	3278.5

Table 3. Numerical comparison between the hybrid algorithm and the GA.

Solution algorithm	GA-MDO-CC	GA
Average energy production (kWh)	1.1426×10^9	1.1168×10^9
Average number of iterations to find first feasible solution	417	838
Average number of iterations to terminate	1267	3000

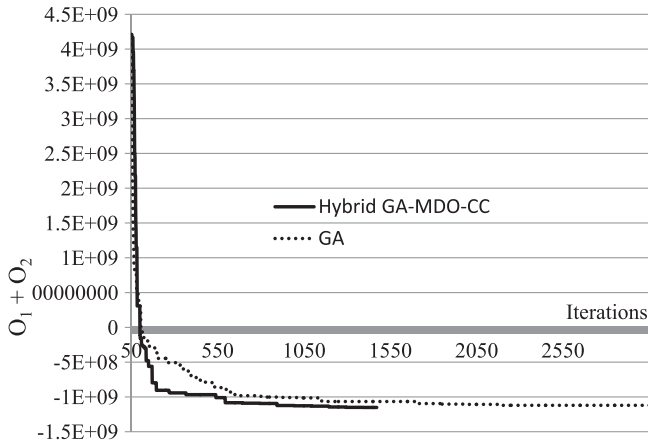


Figure 8. Comparison between convergence paths: hybrid versus GA.

the average number of iterations it took to obtain the first feasible solution are also presented in Table 3.

According to Table 3, the hybrid optimization algorithm generations designs have an average energy production 2.3% higher than those of the designs from the GA. The ideal energy generation, namely 10 times the energy generation of a turbine in the free steam, is 1.1834×10^9 kWh. Therefore, the introduction of the hybridization achieves a 38.61% reduction in wake loss: 3.45% compared with 5.62%. In addition, the hybrid algorithm tends to find feasible solutions quicker; and it can be terminated earlier compared with the GA, when satisfactory solutions are obtained. A typical path of convergence of each algorithm is plotted in Figure 8, where the y-axis represents the sum of the two objectives, *i.e.* the expected energy generation and the constraint violation.

Note that the numerical case study under consideration is relatively tightly constrained; it thus requires relatively fewer turbines and more effective constraint handling. For such a case study, the presented hybrid approach shows improved solution quality and reduced computation time over the GA alone. On the other hand, in cases where the number of turbines is large and spacing is not a critical concern, the incorporation of the MDO-CC approach may not always improve efficiency. This is because the time complexity of the MDO-CC local refinement is generally of a higher order compared to that of the fitness evaluation operation.

The GA is implemented with a population size of 120, a parent set size of 20, a crossover probability of 0.9, a mutation probability of 0.1, and a tournament size of 4. For the hybrid implementation, a maximum number of iterations without improvement equal to 100 is employed; and the local refinement is applied to the 2 best individuals in the elite set. When the GA is executed without local refinement, both the maximum number of iterations and the maximum number of iterations without improvement are set to be 3000, *i.e.* there is no early termination due to premature convergence. The results are generated on the same computer platform and with the same software packages as used for the numerical test on the MDO-CC local refinement algorithm.

When interpreting the optimization results, it should be noted that the reformulation technique does not come free of additional computational expense. As indicated by the numerical results, the presented decomposition-based approach can help improve computational efficiency. However, as the scale of the wind farm increases, the additional computation expense required by the reformulation will increase. For this reason, the authors believe that the reformulation approach is more suitable for relatively tightly constrained (geographically and space-wise) problems. For such problems, the incorporation of the reformulation approach is more likely to improve constraint satisfaction as well as efficiency and effectiveness in general.

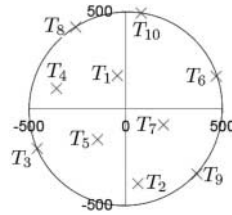


Figure 9. A locally optimal layout of the wind farm case study.

Generally speaking, the computational cost incurred per MPCC solution would increase faster with respect to problem scale than the computation cost of fitness evaluation in GA does. This is because the latter is generally polynomial, while the former is not. Therefore, for large-scale problems where spacing is not of critical concern, the reformulation may not help to improve efficiency in general. But it may still help improve solution quality, especially in the later stages of metaheuristic algorithms, when applied reasonably.

Sensitivity analysis

Note that the two sets of constraints considered in the layout design involve parameters determined in an earlier stage of the wind farm project: the regional constraints depend on the region's radius (or other parameters when some analytical geometric shapes other than circles are addressed); and the inter-turbine spacing constraints depend on the spacing factor α . While these parameters can influence the wind farm layout significantly, their determination may require empirical knowledge as well as considerations beyond the scope of layout design, such as land purchase, environmental impact, maintenance implications, *etc.* In response to this concern, a third numerical study is presented to investigate the effect of these parameters on the wind farm layout design decision. The results may also provide some useful insight into the proper selection of these parameters.

The sensitivity analysis is applied to one of the locally optimal designs obtained with the presented algorithm. The turbine locations (plotted in Figure 9) are given as

$$\mathbf{x} = (-43.65, 170.05, 63.70, -386.27, -456.04, -204.07, -357.78, 103.09, -144.11, -158.42, 466.44, 167.49, 194.46, -82.76, -259.21, 419.77, 368.22, -337.61, 79.69, 493.33)^T. \quad (45)$$

This layout indicates that turbines T_3 , T_8 , T_9 and T_{10} are placed on the boundary of the region and that the inter-turbine spacing constraints are active between T_2 and T_5 , between T_2 and T_9 , as well as between T_7 and T_9 . The Lagrangian multipliers under the negative null form (*i.e.* minimization of the negative of the objective with all constraints converted into less than or equal to constraints) corresponding to the seven active constraints are 135.7106, 6.3072, 135.6525, 148.4861, 63.8596, 158.5221 and 322.4924, respectively.

The effect of region radius on energy production is considered first. Theories relating to Lagrangian multipliers indicate that, if no constraint activity is changed, a small increment ΔR_c in the region radius will result in an additional energy production of

$$-(135.7106 + 6.3072 + 135.6525 + 148.4861)(\Delta R_c^2 + 2R_c \Delta R_c). \quad (46)$$

The MDO-CC approach is applied to the above layout design, with a region radius increased from 500 to 500.2 m. The result indicates an incremental energy production of 8.4972×10^4 kW h, very close to the 8.4096×10^4 kW h suggested by Equation (47).

In a similar manner, the effect of the spacing factor α on the energy production is analysed. The Lagrange multipliers imply that a decrease of $\Delta \alpha$ in α will lead to the following additional

energy production if no constraint activity is changed:

$$-(63.8596 + 158.5221 + 322.4924)(\Delta\alpha^2 + 2\alpha\Delta\alpha)D_0^2. \quad (47)$$

The follow-up optimization results with an α of 3.95, an 0.05 decrement, shows that the expected energy production is increased by $1.2790 \text{ kW} \times 10^5 \text{ h}$, compared with the $1.2877 \times 10^5 \text{ kW h}$ calculated from Equation (47).

A comprehensive consideration of energy production and other factors may lead to a more reasonable determination of the parameters. The sensitivity analysis shown above is made possible by the continuous differentiability of the presented formulation. With this formulation, the parameters' quantitative impact on the objective is directly available in the optimization results. In the absence of a continuously differentiable model, sensitivity analysis will require repeated optimizations under varying parameters, and thus be extremely inefficient. Such a procedure may also be unreliable due to the stochastic nature of current wind farm layout design optimization algorithms.

6. Conclusions

As a result of the wake effect, the layout of turbines in a wind farm has a significant impact on the performance of the farm. However, due to the complexity of wind farm layout design, continuously differentiable optimization models are not available for this problem. This article presented a decomposition-base complementarity model for wind farm layout design optimization. Complementarity constraints were introduced so that the non-smooth wake effect can ultimately be considered in a continuously differentiable optimization formulation; and a decomposed formulation was derived through multi-scenario decomposition. Numerical analysis showed that the presented mathematical program with complementarity constraints (MPCCs) approach effectively generated locally optimal solutions to a test problem and that the presented decomposition-based multi-scenario design optimization with complementarity constraints approach reduced the computation time to obtain locally optimal solutions compared to the all-in-one MPCC approach. The proposed multi-scenario decomposition approach is integrated with a simple bi-objective genetic algorithm (GA) to combine its local optimization capacity with the global exploration capability of the GA. The hybrid algorithm achieved better solutions and reduced computation times compared to the GA, solving a numerical case study which featured a relatively tight boundary constraint that required a relatively tight layout. In addition, sensitivity analysis results on parameter setting changes were able to be derived as a result of the continuous differentiability of the complementarity reformulation.

Funding

The work presented in this article is supported by the National Science Foundation under Award No. CMMI-0900196. Any opinions, findings and conclusions, or recommendations expressed in this publication are those of the authors and do not necessarily reflect the views of the National Science Foundation or Bloomberg LP.

References

- Balling, R. J., and J. Sobieszcanski-Sobieski. 1996. "Optimization of Coupled Systems: A Critical Overview of Approaches." *AIAA Journal* 34 (1): 6–17.
- Bertsekas, D. P. 2003. *Nonlinear Programming*. 2nd ed. Belmont, MA: Athena Scientific.
- Burlaga, L. F. 2000. "Lognormal Distributions and Spectra of Solar Wind Plasma Fluctuations: Wind 1995–1998." *Journal of Geophysical Research* 105 (42): 2357–2364.

- Cassola, F., M. Burlando, M. Antonelli, and C. Ratto. 2008. "Optimization of the Regional Spatial Distribution of Wind Power Plants to Minimize the Variability of Wind Energy Input into Power Supply Systems." *Journal of Applied Meteorology and Climatology* 47 (12): 3099–3116.
- Chen, L., and E. MacDonald. 2011. "A New Model for Wind Farm Layout Optimization with Landowner Decisions." In *Proceedings of the ASME 2011 International Design Engineering Technical Conferences*, 26–31 August, 2011, Washington, DC. New York: ASME.
- Chowdhury, S., J. Zhang, A. Messac, and L. Castillo. 2012a. "Characterizing the Influence of Land Area and Nameplate Capacity on the Optimal Wind Farm Performance." In *Proceedings of the 6th ASME International Conference on Energy Sustainability*, 2012, 23–26 July, San Diego, CA. New York: ASME.
- Chowdhury, Souma, Jie Zhang, Achille Messac, and Luciano Castillo. 2012b. "Unrestricted Wind Farm Layout Optimization (UWFLO): Investigating Key Factors Influencing the Maximum Power Generation." *Renewable Energy* 38 (1): 16–30.
- Christie, David, and Mark Bradley. 2012. "Optimising Land Use for Wind Farms." *Energy for Sustainable Development* 16 (4): 471–475. <http://www.sciencedirect.com/science/article/pii/S0973082612000488>.
- Coello Coello, Carlos A. 2002. "Theoretical and Numerical Constraint-Handling Techniques Used With Evolutionary Algorithms: A Survey of the State of the Art." *Computer Methods in Applied Mechanics and Engineering* 191 (11-12): 1245–1287.
- Corotis, R. B., A. B. Sigl, and J. Klein. 1978. "Probability Models of Wind Velocity Magnitude and Persistence." *Solar Energy* 20 (6): 483–493.
- Couture, T., and Y. Gagnon. 2010. "An Analysis of Feed-In Tariff Remuneration Models: Implications for Renewable Energy Investment." *Energy Policy* 38 (2): 955–965.
- Crespo, A., J. Hernandez, and S. Frandsen. 1999. "Survey of Modelling Methods for Wind Turbine Wakes and Wind Farms." *Wind Energy* 2 (1): 1–24.
- Denholm, Paul, Maureen Hand, Maddalena Jackson, and Sean Ong. 2009. *Land-Use Requirements of Modern Wind Power Plants in the United States*. Tech. Rep. NREL/TP-6A2-45834. Golden, CO: National Renewable Energy Laboratory.
- Du Pont, B. L., and J. Cagan. 2012. "An Extended Pattern Search Approach to Wind Farm Layout Optimization." *Journal of Mechanical Design* 134 (8): 1–18. Paper No. 081002. <http://dx.doi.org/10.1115/1.4006997>.
- European Commission. 1997. "Energy for the Future: Renewable Sources of Energy—White Paper for a Community Strategy and Action Plan." COM(97)599 final (26/11/1997). Accessed November 12, 2013. http://europa.eu/documents/comm/white_papers/pdf/com97_599_en.pdf.
- Frandsen, S., R. Barthelmie, S. Pryor, O. Rathmann, S. Larsen, J. Hojstrup, and M. Thogerson. 2006. "Analytical Modelling of Wind Speed Deficit in Large Offshore Wind Farms." *Wind Energy* 9 (1): 39–53.
- González, Javier Serrano, Angel G. Gonzalez Rodriguez, José Castro Mora, Jesús Riquelme Santos, and Manuel Burgos Payan. 2010. "Optimization of Wind Farm Turbines Layout Using an Evolutive Algorithm." *Renewable Energy* 35 (8): 1671–1681.
- Grady, S. A., M. Y. Hussaini, and M. M. Abdullah. 2005. "Placement of Wind Turbines Using Genetic Algorithms." *Renewable Energy* 30 (2): 259–270. <http://www.sciencedirect.com/science/article/pii/S0960148104001867>.
- Haupt, Randy L., and Sue Ellen Haupt. 2004. *Practical Genetic Algorithms*. Hoboken, NJ: Wiley-Interscience.
- Huang, H. 2007. "Distributed Genetic Algorithm for Optimization of Wind Farm Annual Profits." In *2007 International Conference on Intelligent Systems Applications to Power Systems*, 5–8 November, 2007, Toki Messe, Niigata. Piscataway, NJ: IEEE, 1–6.
- Huang, H. 2009. "Efficient Hybrid Distributed Genetic Algorithms for Wind Turbine Positioning in Large Wind Farms." In *2009 IEEE International Symposium on Industrial Electronics*, 5–8 July, Seoul, Korea. Piscataway, NJ: IEEE. 2196–2201.
- Katic, I., J. Hojstrup, and N. O. Jensen. 1986. "A Simple Model for Cluster Efficiency." In *Proceedings of the European Wind Energy Association Conference and Exhibition (EWEC'86)*, Rome, October 7–9, edited by W. Palz and E. Sesto, Vol. 1, 407–410. Rome: A. Raguzzi for the Italian Section of the International Solar Energy Society.
- Kusiak, A., and H. Zheng. 2010. "Optimization of Wind Turbine Energy and Power Factor with an Evolutionary Computation Algorithm." *Energy* 35 (3): 324–332.
- Kwong, W. Y., P. Y. Zhang, D. Romero, J. Moran, M. Morgenroth, and C. Amon. 2012. "Wind Farm Layout Optimization Considering Energy Generation and Noise Propagation." In *Proceedings of the 2012 ASME International Design Engineering Technical Conferences*, 12–15 August, Chicago, IL. New York: ASME.
- Lackner, M. A., and C. N. Elkinton. 2007. "An Analytical Framework for Offshore Wind Farm Layout Optimization." *Wind Engineering* 31 (1): 17–31.
- Larsen, Gunner Chr., Helge Aagaard Madsen, Niels Troldborg, Torben J. Larsen, Pierre-Elouan Rêhore, Peter Fuglsang, and Søren Ott. 2011. *TOPFARM—Next Generation Design Tool for Optimisation of Wind Farm Topology and Operation*. Forskningscenter Risø, Risø Nationallaboratoriet for Bæredygtig Energi, Risø-R. Danmarks Tekniske Universitet, Denmark.
- Lu, Shen, and Harrison M. Kim. 2010. "A Regularized Inexact Penalty Decomposition Algorithm for Multidisciplinary Design Optimization Problems with Complementarity Constraints." *Journal of Mechanical Design* 132 (4): 1–12. Paper No. 041005. <http://dx.doi.org/10.1115/1.4001206>.
- Lu, Shen, Nathan B. Schroeder, Harrison M. Kim, and Uday V. Shanbhag. 2010. "Hybrid Power/Energy Generation Through Multidisciplinary and Multilevel Design Optimization with Complementarity Constraints." *Journal of Mechanical Design* 132 (10): 1–12. Paper No. 101007. <http://dx.doi.org/10.1115/1.4002292>.
- Lu, S., U. V. Shanbhag, and H. M. Kim. 2008. "Multidisciplinary and Multilevel Design Optimization Problems with

- Complementarity Constraints.” In *Proceedings of the 12th AIAA/ISSMO Multidisciplinary Analysis and Optimization Conference*, 10–12 September, Victoria, BC, Canada, Red Hook, NY: Curran Associates, Inc.
- Luo, Z.-Q., J.-S. Pang, and D. Ralph. 1996. *Mathematical Programs with Equilibrium Constraints*. Cambridge, UK: Cambridge University Press.
- Marmidis, G., S. Lazarou, and E. Pyrgioti. 2008. “Optimal Placement of Wind Turbines in a Wind Park Using Monte Carlo Simulation.” *Renewable Energy* 33 (7): 1455–1460.
- Mosetti, G., C. Poloni, and B. Diviacco. 1994. “Optimization of Wind Turbine Positioning in Large Wind Farms by Means of a Genetic Algorithm.” *Journal of Wind Engineering and Industrial Aerodynamics* 51 (1): 105–106.
- Mustakerov, Ivan, and Daniela Borissova. 2010. “Wind Turbines Type and Number Choice Using Combinatorial Optimization.” *Renewable Energy* 35 (9): 1887–1894.
- Nicks, A. D., and L. J. Lane. 1989. “Weather Generator.” In *USDA Water Erosion Prediction Project: Hillslope Profile Model Documentation*. NSERL Report No. 2, edited by A. D. Nicks and L. J. Lane. 2.1–2.19. West Lafayette, IN: USDA-ARS National Soil Erosion Research Laboratory.
- Rivas, Rajai Aghabi. 2008. “Optimization of Onshore Wind Farm Layouts.” Master’s diss., Technical University of Denmark.
- Skidmore, E. L., and J. Tatarko. 1990. “Stochastic Wind Simulation for Erosion Modeling.” *Transactions of the American Society of Agricultural Engineers* 33 (6): 1893–1899.
- Sobieszczanski-Sobieski, J. 1995. *Multidisciplinary Design Optimization: An Emerging New Engineering Discipline*. Advances in Structural Optimization, 483–496. The Netherlands: Kluwer Academic.
- Takel, E. S., and J. M. Brown. 1978. “Note on the Use of Weibull Statistic to Characterize Wind Speed Data.” *Journal of Applied Meteorology* 17 (4): 556–559.
- Tosserams, S., L. F. P. Etman, and J. E. Rooda. 2007. “An Augmented Lagrangian Decomposition Method for Quasi-Separable Problems in MDO.” *Structural and Multidisciplinary Optimization* 34 (3): 211–227.
- United Nations. 1998. “Kyoto Protocol to the United Nations Framework Convention on Climate Change.” Accessed November 12, 2013. <http://unfccc.int/resource/docs/convkp/kpeng.pdf>.
- Walford, C. A. 2006. “Wind Turbine Reliability: Understanding and Minimizing Wind Turbine Operation and Maintenance Costs.” Report No. SAND2006-1100. Albuquerque, NM: Sandia National Laboratories. Accessed November 12, 2013. <http://www.prod.sandia.gov/cgi-bin/techlib/access-control.pl/2006/061100.pdf>.
- Wan, C., J. Wang, G. Yang, and X. Zhang. 2009. “Optimal Siting of Wind Turbines Using Real-Coded Genetic Algorithms.” In *European Wind Energy Conference and Exhibition (EWEC’09)*, 31 March–3 April, Marseille, France.
- Wan, Chunqiu, Jun Wang, Geng Yang, and Xing Zhang. 2010. “Optimal Micro-Siting of Wind Farms by Particle Swarm Optimization.” In *Advances in Swarm Intelligence*, edited by Ying Tan, Yuhui Shi, and Kay Chen Tan, 198–205. Berlin: Springer.
- WWEA Staff. 2010. “World Wind Energy Report 2010.” In *10th World Wind Energy Conference & Renewable Energy Exhibition—Greening Energy: Converting Deserts into Powerhouses (WWEA2011)*, Cairo, Egypt, October 31–November 2, 2011. Bonn, Germany: World Wind Energy Association.
- Zhang, J., S. Chowdhury, A. Messac, and L. Castillo. 2013. “A Multivariate and Multimodal Wind Distribution Model.” *Renewable Energy* 51 (3): 1324–1332.
- Zitzler, E., and L. Thiele. 1999. “Multiobjective Evolutionary Algorithms: A Comparative Case Study and the Strength Pareto Approach.” *IEEE Transactions on Evolutionary Computation* 3 (4): 257–271.